Homogeneous large-area graphene layer growth on 6*H*-SiC(0001)

C. Virojanadara, M. Syväjarvi, R. Yakimova, and L. I. Johansson
Department of Physics, Chemistry, and Biology, Linköping University, S-581 83 Linköping, Sweden

A. A. Zakharov and T. Balasubramanian
Maxlab, Lund University, S-22100 Lund, Sweden

(Received 13 August 2008; revised manuscript received 18 October 2008; published 1 December 2008)

Homogeneous large-area graphene monolayers were successfully prepared *ex situ* on 6*H*-SiC(0001). The samples have been studied systematically and the results are compared with those from a sample cut from the same wafer and prepared by *in situ* heating. The formation of smaller graphene flakes was found on the *in situ* prepared sample, which is in line with earlier observations. Distinctly different results are observed from the *ex situ* graphene layers of different thicknesses, which are proposed as a guideline for determining graphene growth. Recorded C 1*s* spectra consisted of three components: bulk SiC, graphene (G), and interface (I), the latter being a $6\sqrt{3}$ layer. Extracted intensity ratios of G/I were found to give a good estimate of the thickness of graphene. Differences are also revealed in micro low energy electron diffraction images and electron reflectivity curves. The diffraction patterns were distinctly different from a monolayer thickness up to three layers. At a larger thickness only the graphitelike spot was visible. The electron reflectivity curve showed a nice oscillation behavior with kinetic energy and as a function of the number of graphene layers. The graphene sheets prepared were found to be very inert and the interface between the substrate and the layer(s) was found to be quite abrupt. No free Si could be detected in or on the graphene layers or at the interface.

DOI: 10.1103/PhysRevB.78.245403 PACS number(s): 73.20.−r

I. INTRODUCTION

Silicon carbide (SiC) based electronics has attracted much attention due to its excellent properties for devices operable under extreme conditions.[1] Different metals have been widely selected and intensively studied to improve the metal-SiC interface and device properties. However, silicide formation at the interface and an instability of the metal-SiC devices operating at high temperatures have been observed. Thanks to the SiC composition it is possible to heat the SiC crystal up to elevated temperatures to sublimate the Si atoms and leave a single or few layers of graphene/graphite on top of the substrate. These layers typically have metal character with thickness-dependent properties but also the lateral extent is important.[2] This is crucial for electronic devices since recent studies found that sub-10 nm graphene nanoribbons with smooth edges were obtained and demonstrated to be semiconductors with a band gap inversely proportional to the width.[3] This gives strong motivation to study how to control the thickness and homogeneity of graphene layers to be incorporated into reduced scale devices. Yet, it is still very difficult to prepare a homogeneous large-area graphene layer, and it is unclear under which preparation conditions and at what stage of the high-temperature treatment single layers develop. Although epitaxial growth of graphene on 6*H*-SiC and 4*H*-SiC is actively pursued, achieving large graphene domains with uniform thickness remains a challenge.[4] It is also unknown what actually happens to the Si atoms if some of them remain within the graphene layer or stay on the top of that layer or even remain at the interface.

In this work, we present a successful method to prepare a homogeneous large-area graphene layer. Moreover, we study its quality and indicate the characteristics of layers with different thickness, which may be used as a guideline for graphene growth. The results presented below are obtained from low energy electron microscope (LEEM), photoelectron spectroscopy (PES), angle-resolved photoelectron spectroscopy (ARPES), low energy electron diffraction (LEED), photoemission electron microscope (PEEM), and from micro-LEED and micro-PES at specifically defined small areas.

II. EXPERIMENT

The *ex situ* samples in this study were produced in a prototype of an inductively heated furnace based on the SB generation Epigress heating systems (the Swedish company Epigress is a part of the Aixtron Group) and production grade *n*-type 6*H*-SiC(0001) substrates from SiCrystal with chemical mechanical polishing (CMP) on the Si face, a resistivity of 0.06–0.10 Ω cm, a wafer orientation of $(0 \pm 0.25)^\circ$, and a micropipe density of ≤ 100 cm^{-2} were utilized. This system allows the formation of uniform graphene over a large area. Presently up to 2 in. size substrates are possible in the system. The equipment used for the graphene process has been modified from an earlier version which gave graphitic layers,[5] having qualities which compare quite well with those recorded for natural single crystals. The crucible was specially designed so that the axial and radial temperature gradients were minimized in order to prevent mass transfer from and to the sample. The base pressure in the reactor was 5×10^{-6} mbar. The graphene growth was carried out under highly isothermal conditions at a temperature of 2000 °C and at an ambient argon pressure of 1 atm. The *in situ* sample in this study was prepared by heating the sample resistively to a temperature of 1275 °C for a few minutes at a base pressure of approximately 10^{-10} mbar. The substrate was cut from the same wafer as the *ex situ* prepared samples and pretreated the same way by RCA cleaning (to remove

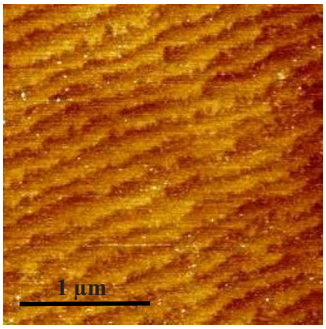

FIG. 1. (Color online) A typical AFM image of the substrate surface before graphene growth showing an average distance between steps of about 0.17 μm.

organic and inorganic contaminations) and HF etching (to remove the surface oxide) to ensure that the initial surfaces were as similar as possible. A representative AFM image of the substrate surface before graphene growth is shown in Fig. 1, illustrating that the average distance between steps is about 0.17 μm. The step height is about 1 nm and the occurrence and direction of the steps are due to the manufacturers misalignment from the nominal on axis orientation.

The number of graphene layers was identified using ARPES, LEED, and LEEM. The as introduced *ex situ* prepared samples showed directly intense $6\sqrt{3}\times 6\sqrt{3}R$ 30° LEED patterns indicating that the surface is very inert and stable under normal atmospheric conditions. Before actual measurements the *ex situ* samples were heated *in situ* at around 700 °C for about a minute and no adsorbed species could then be detected.

Experiments were carried out at the beamline I311 at the MAX synchrotron radiation laboratory. This beamline consists of two end stations. The first station is equipped with a modified SX-700 monochromator[6] and an end station built up around a large hemispherical Scienta electron analyzer[7] which operates at a base pressure of about 1×10^{-10} mbar. The electron analyzer accepts a cone of angular width ±8°. A total-energy resolution, determined by the operating parameters used, of ≤20 meV at a photon energy of 130 eV, of ≤100 meV at 330 eV, and of ≤300 meV at 600 eV was selected in the high-resolution studies of the valence band, Si 2*p* and C 1*s* core levels reported below. The second station is equipped with a spectroscopic photoemission and low energy electron microscope (SPELEEM) instrument. This microscope has a spatial resolution better than 10 nm in the LEEM mode and 30 nm in the PEEM mode. It can also perform energy filtered x-ray photoemission electron microscopy (XPEEM) with a bandwidth of 300 meV in imaging mode, achieving a lateral resolution of 30 nm.

III. RESULTS AND DISCUSSIONS

Figure 1 displays LEEM images of an *ex situ* prepared graphene layer. A homogeneous single domain graphene layer is observed on most part of the sample [as illustrated in Fig. 2(a)]. However, some area consists of two different domains as shown in Fig. 2(b). That it is one layer of graphene was initially identified from the development of the band structure close to the Dirac point, using ARPES. Figure 2(c) shows the recorded π-band dispersion, which is strongly renormalized across the $\bar{K}$ point of the graphite surface Brillouin zone. This is a typical character[8] of monolayer graphene, for which the bands deviate considerably from the expected linear behavior due to many-body interactions. In addition, the LEEM images were recorded as a function of electron energy, and the electron reflectivity was extracted from different areas in the images; details are described below. The reflectivity spectra showed only one dip at an electron energy of around 3 eV, which confirmed that the two different domains both correspond to a single layer of graphene.[9,10]

To identify and distinguish between different numbers of graphene layers, another *ex situ* sample was prepared in the furnace over a longer time, aiming at obtaining more than one layer of graphene. The ARPES results obtained from this sample also showed this to be the case since the π-band dispersion then showed more than one branch around the $\bar{K}$

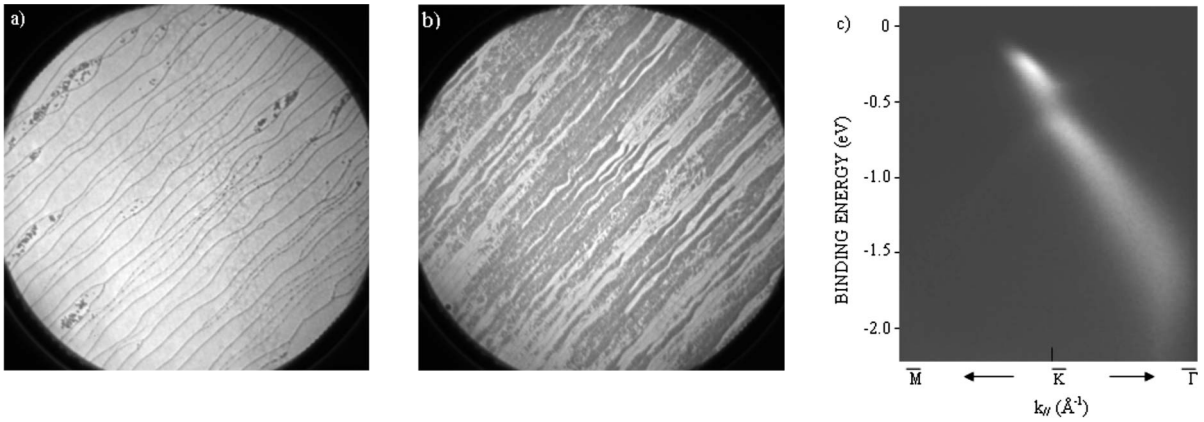

FIG. 2. (a) LEEM image of a single domain monolayer graphene sheet grown *ex situ* on SiC(0001); the FOV is 20 μm and the electron energy is E_{vac}+4.4 eV. (b) LEEM image illustrating the existence of two domains of monolayer graphene; the same voltage and 50 μm FOV is used in this case. (c) Photoelectron intensity map versus binding energy and parallel momentum showing the electronic structure close to the Dirac point at the $\bar{K}$ point of the graphite Brillouin zone.

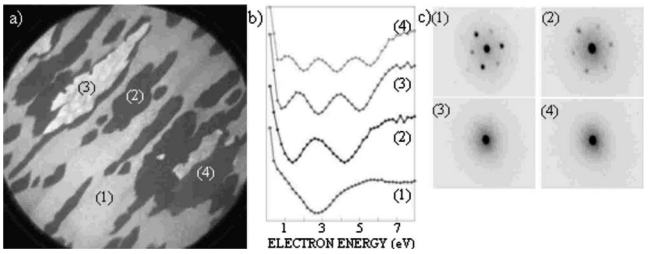

FIG. 3. (a) LEEM image from a second sample grown *ex situ* on which thicker graphene layers were grown; the FOV is 20 μm and the electron energy $E_{vac}+1.6$ eV. (b) Electron reflectivity spectra extracted from the four representative areas [(1)–(4)] corresponding to graphene of 1–4 ML thick, respectively. (c) Micro-LEED collected at $E=53.3$ eV from the four different areas.

point, as expected.[8] A LEEM image of this sample is displayed in Fig. 3(a). The selected region, using a field of view (FOV) of 20 μm, contains areas of different layer thicknesses and the four different areas, marked as (1)–(4), were further investigated. By varying the electron energy the electron reflectivity could be extracted from these four areas and the results are displayed in Fig. 3(b). From area (1) the reflectivity curve shows only one local minimum dip at an energy of around 3 eV, while from the areas marked as (2)–(4) the curve instead exhibits 2–4 dips. Based on earlier observations[9,10] of the variation in the reflectivity with electron energy from graphene samples prepared *in situ*, we can conclude that areas (1)–(4) correspond to graphene with thicknesses of 1–4 layers, respectively. The four selected areas are large enough to allow an investigation of the diffraction pattern originating from the areas of different graphene thicknesses. These micro-LEED results are shown in Fig. 3(c). Interestingly, distinct differences are observed at different layer thicknesses. The graphite related spot is positioned in the middle and its intensity increases with increasing number of graphene layers. Significant changes for the spots around the graphite related spot are also observed which is different compared to earlier findings using conventional LEED.[11] At monolayer graphene thickness (1) the diffraction spots around the graphite related spot show a set of three very intense spots and another set of three spots with much weaker intensity. For two graphene layers (2), the intensity of the first set has become considerably weaker and appears almost similar in intensity compared with the second set of spots. At a thickness of three layers (3) both sets of spots are much weaker but still noticeable. Moreover at a graphene thickness of four layers (4) or more only the graphite related spot is observed. It is worth mentioning that the observed intensity differences may be difficult or impossible to identify using conventional LEED unless a large and homogeneous sample area is provided which has not been possible to obtain so far on samples prepared *in situ*.[9–11] A typical LEEM image from this *ex situ* prepared sample, at a FOV of 50 μm, is demonstrated in Fig. 4(a). The dark stripes show where the growth of a second graphene layer has occurred while the bright areas correspond to growth of one graphene layer. The surface of this sample is thus predominantly covered with one and two layers of graphene but we could find certain regions, such as the one shown in Fig. 3(a), where

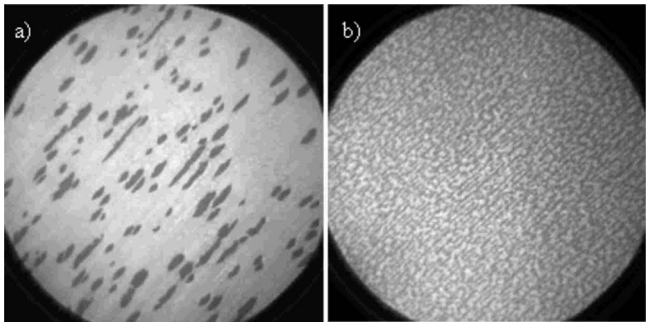

FIG. 4. (a) A typical LEEM image from the second *ex situ* prepared sample showing that the layer coverage is one (bright) and two (dark), predominantly on this sample. The electron energy used is $E_{vac}+4.0$ eV and the FOV 50 μm. (b) An *in situ* prepared sample recorded at an electron energy of $E_{vac}+7.0$ eV and a FOV of 20 μm.

growth of third and fourth layers also had occurred. For comparison a typical LEEM image from the *in situ* prepared sample, at a FOV of 20 μm, is shown in Fig. 4(b). This sample was prepared by resistively heating the SiC crystal *in situ* to about 1275 °C for a few minutes. Only a first layer of graphene has started to develop on this sample as indicated by the darker stripes/spots covering about half the surface area, but interestingly, it is seen to grow in much smaller stripes on the surface. Moreover the width of the elongated dark stripes is about 0.1 μm and the average distance between them is around 0.18 μm, thus essentially the same as the average terrace width on the substrate surface (see Fig. 1). These findings are very similar to earlier reported[9,10,12] LEEM results for *in situ* prepared samples, which also showed that after heating at higher temperatures similar small stripes of two and three layers of graphene developed on the surface. This is a crucial discrepancy between the *ex situ* and *in situ* prepared samples resulting most probably from the different growth conditions playing an important role to control the size of the graphene flakes and layers, respectively. In very recent LEEM and AFM studies[12] of graphene synthesis on SiC(0001) during annealing in vacuum, collected data showed that the surface was rough when graphene formed. The steps were no longer straight and deep pits were observed. Pit formation was traced to the stability of the $6\sqrt{3}$ buffer layer and the existence of gaps in the buffer layer coverage on each terrace. This can explain the formation of the dark stripes/spots observed on our *in situ* prepared surface [Fig. 4(b)]. Rapid nucleation of the buffer layer was suggested[12] to minimize the existence of gaps and to inhibit pit formation. Rapid high-temperature annealing would presumably result in a higher nucleation density with many small closely spaced domains at the steps with smaller gaps between domains and the tendency to form pits would be lower. It was concluded that the growth of smooth flat graphene films may require annealing at temperatures well above 1200 °C, where however multiple layers of graphene may grow[10] when annealing in vacuum. Our *ex situ* samples were prepared at a temperature of 2000 °C in an argon ambient of one atmosphere and produced large domains of flat smooth graphene films. When taking a closer

look at Fig. 2(a) one clearly see steps and terraces and that the average terrace width has changed quite dramatically, from 0.17 to about 0.89 μm (compare with Fig. 1), after the *ex situ* growth. This indicates that the surface morphology is drastically changed after the *ex situ* growth, possibly due to step bunching of the substrate. Much larger terraces have developed and a single layer of graphene has formed on these terraces, as shown in Figs. 2(a) and 2(b). The annealing temperature determines the kinetics of the elements involved. The surface mobility of carbon and the nucleation rate of the buffer layer are expected to increase considerably when raising the annealing temperature from 1200 to 2000 °C. The sublimation rate of silicon, leaving carbon behind, should also increase with temperature. However, the use of a surrounding ambient of Ar, instead of vacuum, is commonly used in sublimation growth experiments to suppress a too fast sublimation rate and provide a smooth decomposition of the SiC. In this particular case it results in both desirable growth and morphology changes, the formation of larger terraces with single layer graphene films on top, as illustrated in Fig. 2. The *ex situ* samples were heat treated in a designed arrangement to minimize the temperature gradient, while the *in situ* sample was heated by running current through it, which may create a thermal gradient in the surface region. Although homogenous sample heating may be of importance for obtaining graphene layers of high quality, our results in combination with the very recent findings[12] suggest that the considerably higher annealing temperature used in combination with an Ar ambient appear to be the key factors for obtaining large homogenous single layer graphene films. A next natural step for the purpose to obtain even wider terraces and thus even larger homogeneous single layer graphene films would be to try similar growth experiments on substrates with better defined on-axis orientation.

It should be noted that our microscopy data from the *ex situ* prepared samples indicate that the second, third, and fourth graphene layers do not appear to develop from a certain position or in a certain direction since the domains observed are rather randomly distributed on and along the large terraces [see Figs. 3(a) and 4(a)]. This observation is different from the recent findings[12] on samples prepared *in situ* where nucleation of graphene was suggested to occur preferentially at steps and in the canyons where the step density was highest. We also attribute these differences to the different growth conditions used for the *ex situ* and *in situ* prepared samples.

The chemical composition of different layers of graphene was investigated using micro-PES, where the signal was averaged over the selected homogeneous area of approximately 1 μm^2. C 1*s* spectra collected using a photon energy of 450 eV from different areas at specified thicknesses using micro-PES are shown in Fig. 5(a). For comparison conventional PES spectra, where the signal is averaged over a much larger selected area (approximately 0.5 mm^2), are shown in Fig. 5(b). It is worth mentioning that the conventional PES spectra were collected at a considerably higher-energy resolution than the micro-PES. Applying a curve-fit procedure shows that the C 1*s* spectra show three components located at binding energies of 283.4, 284.4, and 284.9 eV. These components correspond, respectively, to bulk SiC, graphite/graphene, and the interface (buffer) layers ($6\sqrt{3}$) and are denoted as SiC, *G*, and *I* in Fig. 5. The extracted intensity ratios of (*G*/SiC, *I*/SiC, and *G*/*I*) from micro-PES are (0.8, 1.3, 0.6), (3.0, 1.4, 2.1), and (4.5, 1.7, 2.6) for the thickness of 0.5, 1, and 3 ML, respectively. The ratios obtained from the conventional PES spectra are (1.8, 2.3, 0.7), (3.8, 1.8, 2.2), and (4.7, 1.6, 2.9) for the thickness of 0.5 and 1 and the mixture of 1–4 ML (labeled 1 and 2 ML since that is the predominant layer coverage determined from LEEM), respectively. The ratios obtained from both methods are quite similar, especially the *G*/*I* ratio and for the thickness from 1 ML and larger. This can also be used as a guideline for *in situ* graphene preparation.

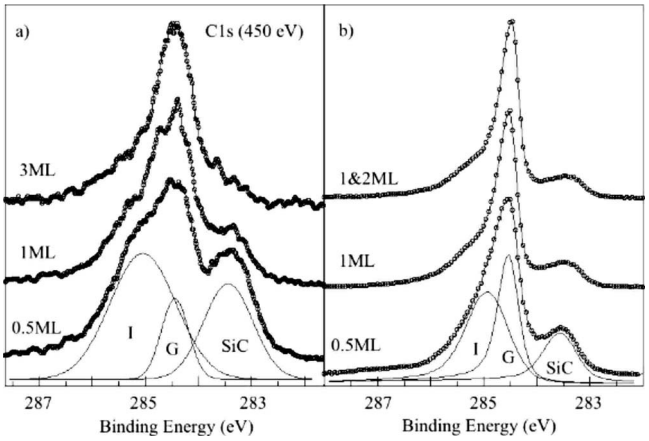

FIG. 5. C 1*s* spectra collected using a photon energy of 450 eV at different graphene thicknesses using (a) micro-PES and (b) conventional PES. Peaks underneath show the components obtained when applying a fitting procedure. The 0.5 ML spectra where collected from the *in situ* prepared sample, while the other spectra were collected from the *ex situ* prepared samples.

Typical C 1*s* and Si 2*p* spectra collected from the homogeneous large-area single graphene layer sample (see Fig. 2) at different photon energies are displayed in Figs. 6(a) and 6(b), respectively. It is very interesting to point out that the bulk SiC signal in the C 1*s* spectrum collected at the photon energy of 330 eV is not possible to detect already after a single layer of graphene has developed [Fig. 6(a)]; but on the contrary, the bulk SiC signal of the Si 2*p* spectrum collected at the photon energy of 140 eV in Fig. 6(b) is very sharp and intense although the electron escape depth of these core levels at the specified energies is similar, i.e., approximately 3 Å.[13] This rises an interesting question concerning what has actually happened to the Si when the graphene sheet(s) is grown. Can the Si atoms be mixed within the graphene sheet, in between the layers, or even cluster on the outermost layer? However, in the Si 2*p* spectra no component at a binding energy of 99 eV could be detected and this indicates that no Si-Si bond component exists in or on the graphene layer(s) grown. The PEEM image (E_{kin}=24 eV, E_b=101 eV) shown in Fig. 7, recorded from the *ex situ* prepared sample over essentially the same selected area as displayed in Fig. 3(a), shows a weaker Si 2*p* signal where thicker graphene layers have grown, i.e., area (4) darkest and area (1) brightest. This indicates a Si containing region close to the first graphene layer but not on top of the graphene layers. There-

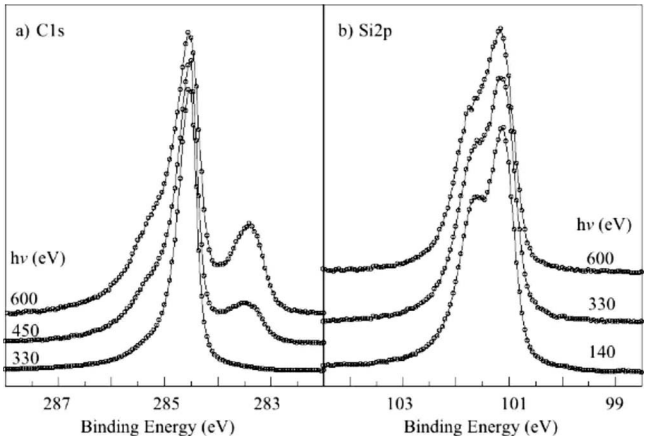

FIG. 6. Conventional PES of the (a) C 1*s* and (b) Si 2*p* core levels collected from the *ex situ* prepared homogeneous single graphene layer sample using different photon energies.

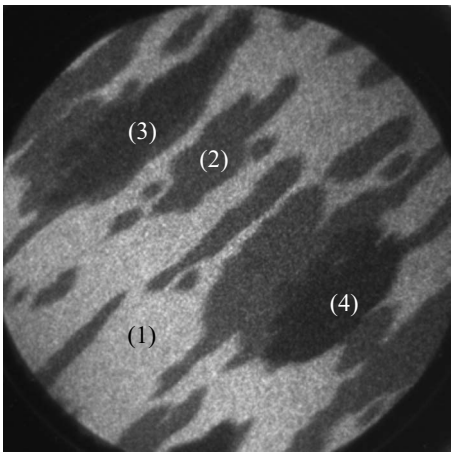

FIG. 7. A PEEM image obtained using the Si 2*p* level and collected at a photon energy of 130 eV. The image shows essentially the same selected region as in Fig. 2(a) so the different selected areas (1)–(4) are identified and the relative intensity from layers of different thicknesses can be compared.

fore we can conclude that the extra sharp Si 2*p* "SiC bulk-like" signal originates from Si atoms within the interface (buffer) layer, including the Si atoms in the topmost SiC bilayer, and located very close to the graphene layer, which has metallic properties. This affects the spectral shape in the Si 2*p* core level and produces a very sharp and well-separated spin-orbit split peak compared to the typical bulk-truncated SiC surface.[14]

IV. SUMMARY

Using surface characterization methods we demonstrate an *ex situ* method for growth of large and homogeneous areas of single layer graphene on top of a SiC(0001) substrate. Our results show that single domain graphene is formed over quite large areas but that two different domains existed on some parts of the sample. Comparison was made with an *in situ* prepared graphene sample yielding similar results as earlier published:[9,10,12] that the size of the graphene flakes then were very small compared to those obtained from the samples prepared with the *ex situ* method. Possible explanations for the formation of the larger homogeneous graphene layers using the *ex situ* preparation method were discussed. Micro-LEED images collected from the *ex situ* sample prepared to have different graphene thicknesses showed distinct differences in the diffraction pattern. Recorded C 1*s* spectra consisted of three components and extracted intensity ratios from micro-PES and conventional PES were found to give a good estimate of the thickness of the graphene layer. The substrate is suggested to terminate with an interface layer containing Si atoms located closely to the graphene layer, resulting in a very sharp Si 2*p* signal where the spin-orbit splitting is much better resolved than from typical bulk-truncated SiC surfaces.

The present results open up possibilities and opportunities for graphene-SiC based electronic devices since the preparation of a large-area and homogeneous monolayer graphenes is now possible. This has been the main obstacle so far. Surface patterning lithography of this large-area graphene is possible since the graphene surface is very inert in the atmospheric ambient and has good chemical resistance. Due to its intriguing electronic properties, graphene is also of interest to use in sensor applications in studies of adsorption phenomena ranging from atoms to biomolecules.

ACKNOWLEDGMENTS

Support from the European Commission under the Marie Curie Intra-European fellowship action (EIF) and the Swedish National Energy Administration are gratefully acknowledged.

[1] S. E. Saddow and A. Agrawal, *Advances in Silicon Carbide Processing and Applications* (Artech House, London, 2004).
[2] A. Bostwick, K. V. Emtsev, K. Horn, E. Huwald, L. Ley, J. L. McChesney, T. Ohta, J. Riley, E. Rotenberg, F. Speck, and Th. Seyller, Adv. Solid State Phys. **47**, 159 (2008).
[3] X. Wang, Y. Ouyang, X. Li, H. Wang, J. Guo, and H. Dai, Phys. Rev. Lett. **100**, 206803 (2008).
[4] W. A. de Heer, C. Berger, X. Wu, P. N. First, E. H. Conrad, X. Li, T. Li, M. Sprinkle, J. Hass, M. L. Sadowski, M. Potemski, and G. Martinez, Solid State Commun. **143**, 92 (2007).
[5] T. Kihlgren, T. Balasubramanian, L. Walldén, and R. Yakimova, Phys. Rev. B **66**, 235422 (2002).
[6] R. Nyholm, S. Svensson, J. Nordgren, and S. A. Flodström, Nucl. Instrum. Methods Phys. Res. A **246**, 267 (1986).
[7] J. N. Andersen, O. Björnholm, A. Sandel, R. Nyholm, J. Forsell, L. Thånell, A. Nilsson, and N. Mårtensson, Synchrotron Radiat.

News **4**, 15 (1991).
[8] T. Ohta, A. Bostwick, J. L. McChesney, Th. Seyller, K. Horn, and E. Rotenberg, Phys. Rev. Lett. **98**, 206802 (2007).
[9] H. Hibino, K. Kagashima, F. Maeda, M. Nagase, Y. Kobayashi, and H. Yamaguchi, Phys. Rev. B **77**, 075413 (2008).
[10] T. Ohta, F. El Gabaly, A. Bostwick, J. L. McChesney, K. V. Emtsev, A. K. Schmid, Th. Seyller, K. Horn, and E. Rotenberg, New J. Phys. **10**, 023034 (2008).
[11] C. Riedl, U. Starke, J. Bernhardt, M. Franke, and K. Heinz, Phys. Rev. B **76**, 245406 (2007).
[12] J. B. Hannon and R. M. Tromp, Phys. Rev. B **77**, 241404(R) (2008).
[13] P. J. Cumpson and M. P. Seah, Surf. Interface Anal. **25**, 430 (1997).
[14] L. I. Johansson, F. Owman, and P. Mårtensson, Phys. Rev. B **53**, 13793 (1996).